ОБЪЕДИНЕННЫЙ
ИНСТИТУТ
ЯДЕРНЫХ
ИССЛЕДОВАНИЙ

Дубна

99-225

E14-99-225

S.A.Karamian[1], W.Assmann[2], K.Ertl[3], D.Fritschke[2],
H.D.Mieskes[2], B.Schmidt[4], S.P.Tretyakova

CAPTURE FROM A RANDOM FLUX TO THE CHANNELING FOR PROTONS TRANSMITTED THROUGH A Si FOIL

Submitted to the 18th International Conference
on Atomic Collisions in Solids, August 1990, Odense, Denmark

[1]Corresponding author E-mail: karamian@cv.jinr.dubna.su
[2]Sektion Physik, Ludwig-Maximilians-Universität, München, D-85748, Garching, Germany
[3]Max Planck Institut für Plasmaphysik, D-85748, Garching, Germany
[4]Forschungszentrum Rossendorf, D-01314, Dresden, Germany

1999

Карамян С.А. и др. E14-99-225

Захват в каналирование из случайного потока протонов, проходящих через Si фольгу

Для протонов, проходящих через монокристаллическую мембрану из Si, наблюдено перераспределение потока и формирование пиков каналирования в геометрии, когда частицы имели исходно широкое угловое распределение. Пики каналирования продуцируются кристаллической средой в результате многократной перезарядки иона вследствие зависимости сечений подхвата и потери электрона от прицельного параметра. Это объясняет наблюдение пиков каналирования только при достаточно низкой остаточной энергии протонов после прохождения: $E_p^f \leq 0{,}6$ МэВ.

Работа выполнена в Лаборатории ядерных реакций им. Г.Н.Флерова ОИЯИ.

Препринт Объединенного института ядерных исследований. Дубна, 1999

Karamian S.A. et al. E14-99-225

Capture from a Random Flux to the Channeling for Protons Transmitted through a Si Foil

Flux redistribution and formation of channeling peaks have been observed in the geometry of initially wide-angle incidence for protons transmitted through monocrystalline Si membranes. The channeling peaks are generated by the crystalline medium as a result of multiple charge-exchange events due to the impact-parameter dependence of the electron capture and loss cross sections. This explains successfully the detection of channeling peaks only at a low enough residual proton energy: $E_p^f \leq 0.6$ MeV, after the transmission.

The investigation has been performed at the Flerov Laboratory of Nuclear Reactions, JINR.

Preprint of the Joint Institute for Nuclear Research. Dubna, 1999

1. Introduction

A flux of particles uniformly distributed both by the angle and space coordinates should remain being uniform after its transmission through a crystal. Some group of particles can be channeled due to the low transverse energy in incidence, but that doesn't create any crystallographic modulation of the flux because of the uniform spectrum of the transverse energy. This is related both to the potential Liouville motion when the inelastic processes are neglected and to the case when electronic energy losses are taken into account. Transverse energy fluctuations have to be reversible as predicted by the basic theory [1].

Experimentally the "channelography" patterns were detected as early as indicated in refs. [2,3] using a uniform flux of α-particles from radioactive sources. The result was explained by the experimental conditions providing the energy-loss discrimination, and, thus, the selection of the group of channeled particles. This is similar to the "in-beam" experiments [4,5] where the lowest energy losses could be selected for protons scattered at a large angle in a semi-thick crystal target. With such a discrimination the channeling maxima were detected clearly, despite the channeled group being low in intensity, and a blocking pattern of a remarkable contrast was observed without any special selection. The channeling maxima were also detected [6-8] in the small-angle scattering experiments within the multiple-scattering spot of the beam, whereas normal blocking corresponds to the range of large angles. The results [6-8] are again explained by the selection of the higher energy particles due to the use of photoplate detectors, and also by the reduction of the flux density at all random directions due to the multiple-scattering spread. The latter reason is lower in efficiency for the channeled fraction.

Объединенный институт
ядерных исследований
БИБЛИОТЕКА

For heavy ions, the reflection patterns were systematically recorded in experiments [9,10] using solid-state track detectors in a standard blocking geometry. The reverse of the pattern contrast from blocking to channeling was unexpectedly revealed when particles were emitted from the depth of 5-10 μm of a crystal. This observation was confirmed in ref. [11], when the scattered ions (recoils) were detected with a good depth-resolution using a position-sensitive ionization chamber. However, the explanation of such a transformation of the pattern was not found.

The complete de-channeling is normally deduced from the RBSC spectra at considerable depths. However, they may mean only that the deep layer yield becomes insensitive to the initial beam de-orientation, while the real flux distribution at considerable depths remains hidden. Thus, the equilibrium flux distribution after a long enough path in the crystal should be studied in special experiments.

For the detection of the uniform flux redistribution the standard geometry of a collimated beam does not provide the right initial condition. The beam uniformly fills the interatomic spaces at the entrance into the crystal, but there is a narrow peak in the momentum coordinates. So, the capture into channeling is absolutely natural for the particles directly from the beam or after the small-angle scattering. In contrast, the wide-angle random flux is created by the Rutherford scattering in the crystal, but it is not uniform in the space distribution. All scattered at a large angle particles are emitted from the cites, and, thus, the blocking distribution ought to be created.

In order to reach the really uniform flux distribution both in the space and momentum coordinates a new geometry has been proposed and applied in ref. [12] for heavy ions. The functions of the scatterer and the transmitted crystal layer are separated. The beam hits some polycrystalline target, and the scattered particles on the way to the detector have to cross a monocrystalline layer. In the present work such geometry is applied to the detection of the crystal-induced flux modulation for protons in Si.

2. Experimental

The experiment was performed at the 2.5 MV accelerator of the Institute of Plasma Physics at Garching; the geometry is schematically shown in Fig.1. The proton beam after passing through a 0.8 mm aperture was directed to a thin (100 $\mu g/cm^2$) Au target. The scattered protons crossed the Si layer and stopped in a CR-39 plastic track detector located at 120° in the scattering angle. The monocrystalline Si membranes, 8.7 or 2.3 μm in thickness and of the (100) orientation were placed between the detector and the scatterer, quite close to the latter, but out of the reach of the beam. That prevented any damage and distortion of the foil under irradiation.

The thin Si membranes were prepared using the technology described in ref. [13]. After preparation, the membranes were thermally annealed, and their perfect monocrystalline structure was confirmed in many control tests detecting the blocking and channeling patterns using the ERDA set-up [14] on the heavy ion beams of the Muenchen Tandem. The "dimpling" distortion of the foils by the beam was also clearly established.

In the present experiment the virgin non-irradiated membranes were used. Such foils are quite flexible (being fragile) and can be distorted by any insignificant strain applied to the frame under assembling, or even due to oxidization of the surface. So, all the operations were fulfilled with caution, as well as the etching of the foil could be repeated in the case the oxidization strain appeared.

In the described geometry the crystal was exposed to a low intensity random (both by angles and coordinates) flux of scattered protons. The scattering angular distribution was flat within the solid angle covered by the detector, ± 4° in both directions. The trajectories of scattered protons were not restricted by any collimators in the direction onto the detector. The multiple scattering in the Si degrader mixed the angles without reducing the flux density since the departing protons were replaced by the coming-in ones. The distance between the crystal and the detector was 275 mm providing the angular resolution of about 0.08°. A good resolution was necessary for the detection of the crystallographic pattern, if created.

After the exposure the detector plate was etched in a 20% NaOH solution at 70°C in order to develop the proton tracks. As known, CR-39 detectors are sensitive to protons in the range from the tens of keV up to a few MeV. The detection efficiency (at normal incidence) is nearly 100%, since each proton produces one track, and the diameter of the track is more or less stable at energies near the maximum of the energy loss. At high enough density of tracks on the detector surface, the recorded pattern can be visualized after etching. In our experiments a crystallographic image was clearly observed when the residual proton energy was below 0.6 MeV. An example of this is shown at the photo in Fig.2. This crystallographic pattern is formed by the lines and spots of enhanced intensity in the direction of the planes and axes due to channeling.

3. Results

The described conditions met the requirement of the really wide-angle random distribution of particles uniformly filling the interatomic space in the crystal lattice. Also there was no energy-loss selection for the particles detected at the exit from the crystal. In all irradiations the thickness of the Si degrader was significantly lower than the proton range in a random direction. Thus, after transmission the protons had the energy enough to produce tracks on the detector surface. The detector response was proportional to the number of particles, and not to their energy as is the case with photoplates. Definitely, it is the real flux enhancement and not the energy contrast that was detected in the present work for p transmitted through Si, see Fig.2.

The number of tracks on the detector surface was counted using an optical microscope, and the coordinate dependence of the track density was scanned to characterize quantitatively the observed structures. The results taken for the <100> Si axis are given in Fig.3. The position coordinate has been re-calculated into the angle of de-orientation from the axis, and the relative yield, χ, has been normalized to the track density at random directions. One can see in Fig.3 the channeling peaks in the axial direction accompanied by the negative (χ < 1.0) shoulders. The angular width of peaks appeares to be below the Lindhard angle value, typically it was about 0.5 ψ_1, provided ψ_1 is calculated for the residual energy E_p^f of protons.

The beam energy was varied from 0.45 to 1.0 MeV, and with the crystals 2.3 and 8.7 μm in thickness the range of E_p^f = (0.12-0.60) MeV was covered. The latter values were calculated using the random energy losses of p in Si. The peak and shoulder amplitudes in Fig.3 are definitely dependent on E_p^f.

In Fig.2 the (110) and (100) planar reflections are also prominent. For quantitative presentation the scanning results are given in Fig.4 for the (110) plane at two values of E_p^f. In general, the planar peaks are lower in intensity than the axial ones, and the (100) image is not so contrast as the (110) one. For the latter direction intense shoulders are also typical, see Fig.4.

Below one can find a general scheme within which we try to explain the appearance of the channeling peaks and their energy dependences. However, the quantitative description of the peak amplitude, its shape and dependence on the Miller indexes has not yet obtained.

4. Discussion

Channeling peaks detected here and in [12] are in agreement with the earlier observations [9-11]. At the same time, the conditions of the present experiment and observed properties prove that the origin of the effect is quite different from that discussed in refs. [15] and [16]. Indeed, the volume capture of protons to channeling in bent crystals was discussed in [15] for energies in the range of GeVs. However, in our case the channeling peaks are deteriorating at $E_p^f \geq 0.6$ MeV. In ref. [16] some energy contrast was created by the stacking fault defects inserted artificially into the Si crystal before the proton microprobe experiment. In our case, the real flux modulation is detected when the virgin crystal is placed out of the beam reach. Thus, the modulation can be attributed neither to the energy-loss selection, nor to the crystal damage. As described in the Introduction, other experiments [2-8] were explained successfully within a standard theoretical approach. Unlike [2-8,15,16], the results of refs. [9-12] and those of the present work require some new mechanism for their understanding, since they seem to contradict the reversibility principle which is basic in theory.

From Figs.3 and 4 one can conclude that the amplitude of a channeling peak is defined mostly by the residual energy E_p^f of protons. Our crystals were, obviously, thick enough (even 2.3 μm ones) to create the equilibrium distribution of particles, and similar patterns were observed for different thicknesses, if the E_p^f value was the same. On the contrary, the variation of E_p^f changes significantly the observed pattern. At E_p^f = (0.4-0.5) MeV the central peak is not high in amplitude, and the negative (< 1.0) shoulders are pronounced. At low energy E_p^f = (0.1-0.2) MeV the flux in the central peak exceeds the random value by as many as 25%, whereas the shoulders are not pronounced. The E_p^f dependence of the pattern is in agreement with the results obtained for ^{4}He and ^{12}C ions in ref. [12], in which the peak amplitude decreasing with the growth of the ion residual energy was also observed.

Such regularity can serve as a probe for any explanation of the observed flux modulations. A new mechanism has been proposed in ref. [17] and developed in [12] for the understanding of the cooling (heating) of the transverse momentum distribution due to the electron capture and loss processes. The impact-parameter dependence of the charge-exchange cross-sections provides the ion trajectory cooling (heating) if the electron capture (loss) is predominant within short distances.

In Fig.5 the stopping power curves for charged particles in Si are shown (ref. [18]), the horizontal arrows point at the energy ranges, where the channeling peaks are observed for protons, alphas and ^{12}C - ions. One can see the same position of the upper limit for all the ion species with respect to the corresponding stopping curve, namely, near the energy where the stopping begins to be E^{-1} dependent. This energy corresponds to the effective stripping of the last electron from a projectile, and, thus, to the deterioration of the charge-exchange processes. The channeling peaks disappear at these energies, so their correlation with the charge-exchange processes is confirmed in accordance with the mechanism proposed in ref. [17].

After an elementary event of the electron capture, the potential part of the particle transverse energy $E_\perp$ is decreased proportionally to $(Z_1 - 1)/Z_1$, and then $E_\perp$ is partially recovered when the electron is lost again. Finally, the mean $\Delta E_\perp$ value is negative if the capture process predominates at short distances and the loss - at long distances. Such scenario is realized for light and medium mass ions. Decreased $E_\perp$ leads to the compression of the particle-emission angles and to the formation of peaks of intensity at axial and planar directions. Thus, the impact-parameter dependence of the capture-to-loss ratio of the cross-sections is responsible for the effect.

The absolute values of the cross-sections are also important. This mechanism is inefficient when quite a few capture events occur during the transmission through the crystal layer. In addition, a very high electron-loss cross-section also excludes the effective cooling. Indeed, when the capture and the loss occur practically in the same point, no change of the potential energy takes place. Therefore, one has to estimate the free pathlengths l_{capt} and l_{loss} for the capture and the loss, respectively, and to compare the former with the crystal thickness t and the latter with the channeling trajectory wave-length λ.

The sinusoidal trajectory of planar channeling is characterized in the harmonical approximation by:

$$\lambda = \frac{2\pi A}{\psi_c}, \qquad (1)$$

where A is the maximum amplitude of oscillations, and ψ_c is the critical angle of planar channeling. On the pathlength λ/4 the potential energy varies from maximum to zero. Thus, l_{loss} should be compared with λ/4. For axial channeling the trajectory is not sinusoidal, however, the longitudinal parameter of the trajectory can be estimated by analogy using equ. (1). We assume that $A = a / 2\sqrt{2}$ for the <100> Si channel and $\psi_c = \psi_1$.

In order to find the realistic values of the capture and loss cross-sections and estimate l_{capt} and l_{loss}, empirical information has been used which is available in refs. [19-22]. The empirical formula proposed in ref. [19] yields more or less reliable cross-sections, however, we also apply additional calibration of the cross-section, separately for protons, alphas and C-ions using the measured values [20-22]. The results are summarized in Table 1. At all energies, where the channeling peaks are detected, the inequality:

$$\frac{l_{capt}}{t} \ll 1, \qquad (2)$$

is fulfilled, whereas the ratio of l_{loss} and λ/4 is varied:

$$0.05 \leq \frac{4 l_{loss}}{\lambda} \leq 4. \qquad (3)$$

The absolute values of these ratios do not exclude that the charge-exchange mechanism is responsible for the observed channeling peaks. Moreover, the correlation of the l_{capt} and l_{loss} parameters with the variation of the channeling peak amplitude taken for different ion species at different energies can be seen in Table 1. This confirms the validity of the discussed mechanism for the explanation of the flux re-distribution in a crystalline medium.

Unfortunately, the empirical data do not provide sufficient information for describing the impact-parameter dependence of the cross-section in crystals and for predicting quantitatively the intensity of channeling peaks. An advanced theoretical model is required to describe the charge-exchange processes for ions in crystals, as well as to simulate the trajectories of the charge-fluctuating ions.

5. Summary

According to theoretical predictions, the wide-angle random distribution of particles remains random after transmissing through a monocrystalline layer due to the reversibility of the transverse-energy fluctuations. In the present experiment the requirements of the wide-angle incidence flux and of the absence of any selection of transmitted particles by energy-loss are fulfilled. The channeling enhancement of the flux has been revealed for protons transmitted through Si layers when the residual energy has been kept in a range of (0.1-0.6) MeV. A conclusion is drawn that the orientation modulation of the flux is generated by the inelastic charge-exchange processes in crystals, and it is explained by the impact-parameter dependence of the electron capture and loss cross-sections.

6. Acknowledgments

The authors gratefully acknowledge numerous valuable discussions with J.U.Andersen (Aarhus University) and R.Behrisch (MPI/IPP Garching) as well as the support from H.J.Maier, M.Schmidl and F.Schmidt in supplying scattering targets, beam operations and photography of detected images. One of us (S.A.K) is grateful to the DLR IB/OVB office (Germany) for the support of the JINR-LMU collaboration.

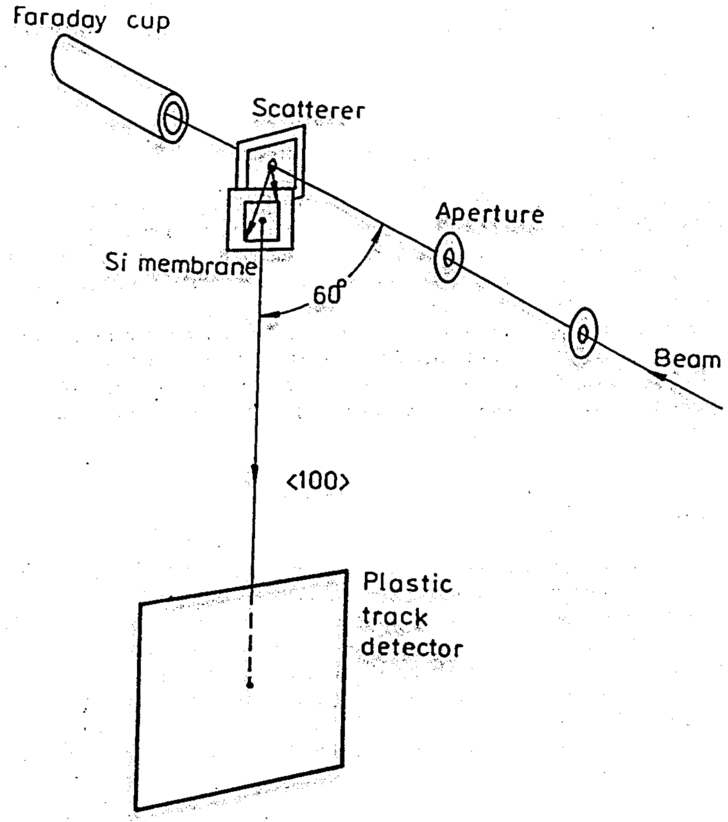

Fig.1. Schematic diagram of the experimental setup.

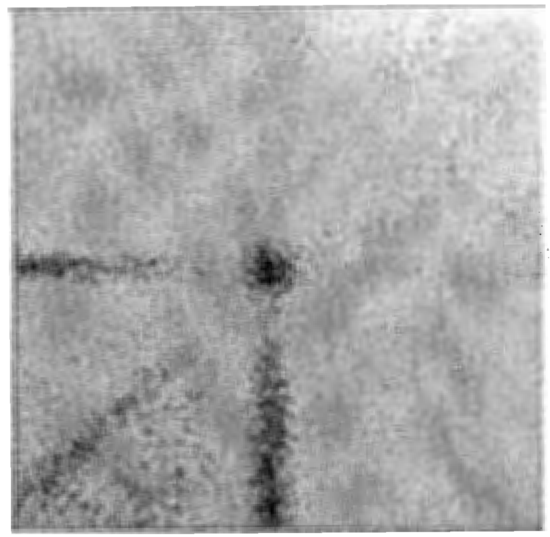

Fig.2. A photo of the "channelography" image recorded by a CR-39 track detector at $E_p^f = 0.28$ MeV. The contrast is reversed to show higher density of tracks by more dense areas.

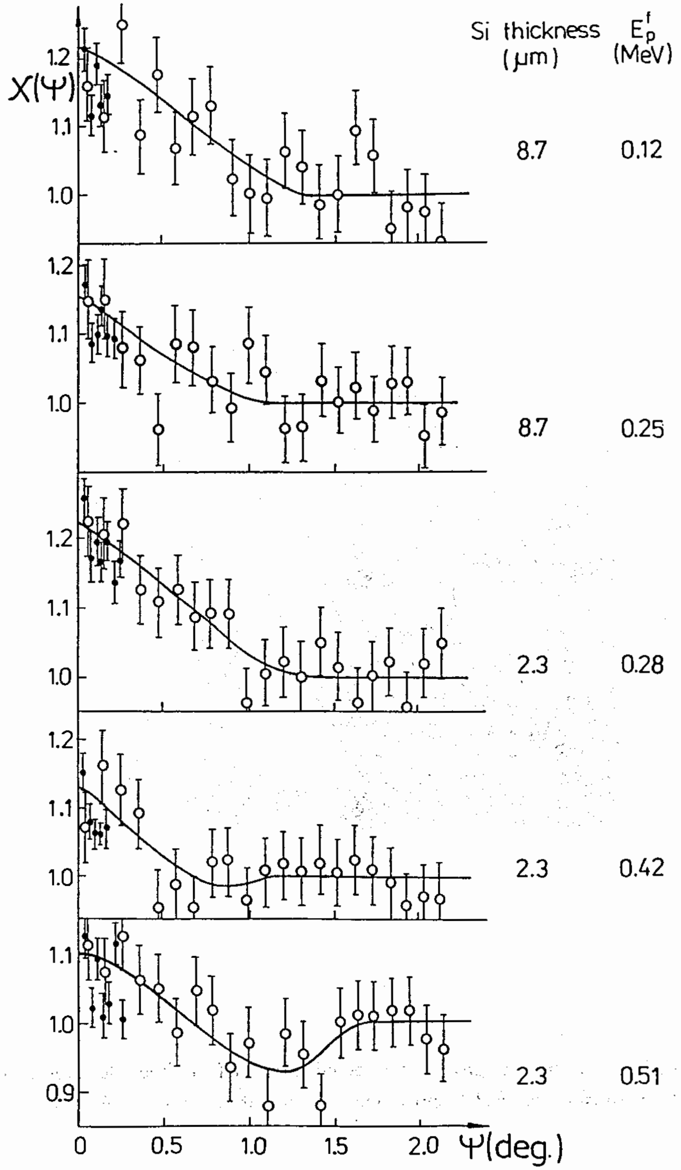

Fig.3. The orientational dependences generated by the <100> axis of Si at different thicknesses and E_p^f values (indicated in the Figure). Linear scan results (o) are combined with circular scan ones (•) near the maximum; the solid line is the guideline.

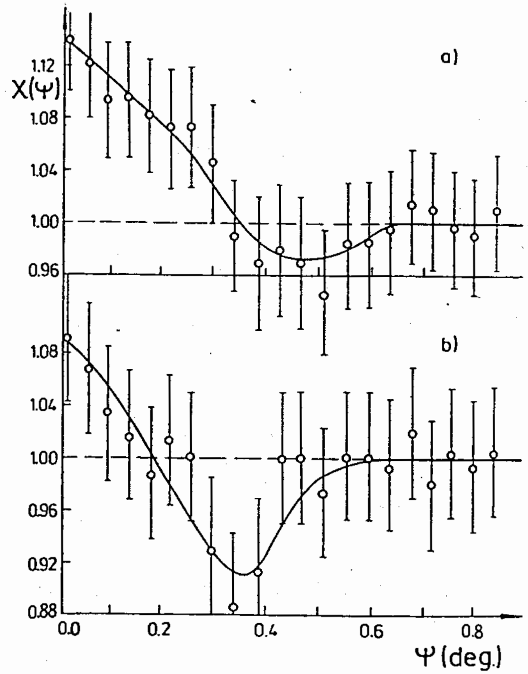

Fig.4. The same as in Fig.3, but measured for the (110) plane of the Si crystal (2.3 μm thickness) at E_p^f = 0.28 and 0.51 MeV, a and b, respectively.

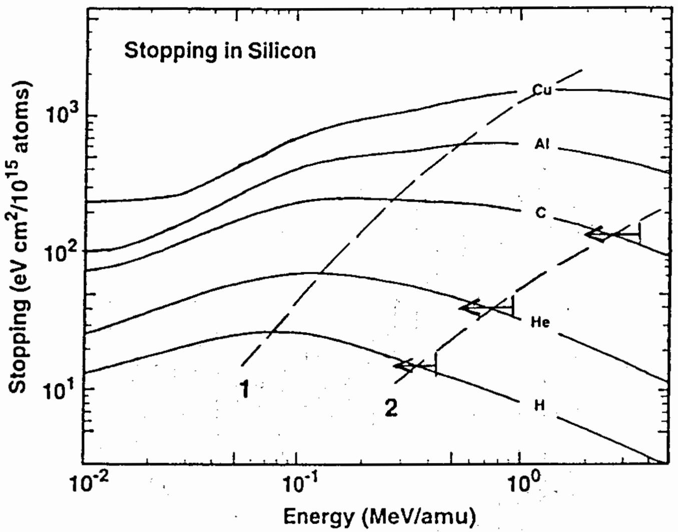

Fig.5. Energy-loss curves for heavy ions in Si as given in ref. [18]. For ^{1}H, ^{4}He and ^{12}C the energy range within which the capture into channeling could be detected is shown by the horizontal arrow. Dashed curves (1 and 2) show a parallel shift of the arrows from the positions of the stopping maxima.

Table 1. Measured and calculated parameters describing the capture of particles into channeling in a Si crystal.

Particle	Exit energy (MeV)	Crystal thickness (μm)	χ_{max}	Free path length (μm) l-capture	Free path length (μm) l-loss	λ/4 (μm)
^{1}H	0.28	2.3	1.24 ± 0.05	0.12	$0.8 \cdot 10^{-3}$	$1.8 \cdot 10^{-2}$
	0.42	2.3	1.13 ± 0.05	0.32	$1.1 \cdot 10^{-3}$	$2.2 \cdot 10^{-2}$
	0.51	2.3	1.10 ± 0.05	0.74	$1.2 \cdot 10^{-3}$	$2.5 \cdot 10^{-2}$
^{4}He	1.7	8.7	1.32 ± 0.05	$2.1 \cdot 10^{-2}$	$2.8 \cdot 10^{-3}$	$3.2 \cdot 10^{-2}$
	3.1	8.7	1.18 ± 0.05	$8.7 \cdot 10^{-2}$	$4.3 \cdot 10^{-3}$	$4.3 \cdot 10^{-2}$
^{12}C	15	8.7	1.50 ± 0.07	0.14	0.20	$5.3 \cdot 10^{-2}$
	25	8.7	1.22 ± 0.05	0.56	0.22	$7.1 \cdot 10^{-2}$
	35	8.7	≤ 1.05	1.3	0.25	$8.5 \cdot 10^{-2}$

7. References

1. J. Lindhard, Det. Kongl. Dan. Vid. Selsk. Mat.-fys. Medd. 34 (1965) No. 14.
2. Y. Quere, H. Couve, J. Appl. Phys. 39 (1968) 4012.
3. V.V. Skvortsov, I.P. Bogdanovskaya, Pis'ma Zh. Eksp. Teor. Fiz. 11 (1970) 1.
4. D.S. Gemmel, R.E. Holland, Phys. Rev. Lett. 14 (1965) 945.
5. F. Fujimoto, K. Komaki, M. Maruyama, K. Tsukada, K. Ozawa, M. Mannami, T. Sakurai, Phys. Stat. Sol. a 4 (1971) 485.
6. G. Dearnaley, I.V. Mitchell, R.S. Nelson, B.W. Farmery, M.W. Thomson, Phil. Mag. 18 (1968) 985.
7. B.R. Appelton, L.C. Feldman, Rad. Eff. 2 (1969) 65.
8. G. Della Mea, A.V. Drigo, S. Lo Russo, P. Mazzoldi, G.G. Bentini, S.U. Campisano, G. Foti, E. Rimini, Nucl. Instr. and Meth. 132 (1976) 163.
9. S.A. Karamian, Izv. Akad. Nauk SSSR, Ser. Fiz. 51 (1987)1008.
10. S.A. Karamian, Nucl. Instr. and Meth. B 51 (1990) 354.
11. H. Nolte, W. Assmann, H. Huber, S.A. Karamian, H.D. Mieskes, Nucl. Instr. and Meth. B 136-138 (1998) 587.
12. W. Assmann, Invited talk on the present Conference.
13. B. Schmidt, J. von Borany, U. Todt, A. Erlebach, Sensors and Actuators A 41-42 (1994) 689.
14. W. Assmann, J.A. Davies, G. Dollinger, J.S. Forster, H. Huber, T. Reichelt, R. Sigele, Nucl. Instr. and Meth. B 118 (1996) 242.
15. V.A. Andreev, V.V. Baublis, E.A. Damaskinski, A.G. Krivschich, L.G. Kudin, V.V. Marchenkov, V.F. Morozov, V.V. Neliubin, E.M. Orischin, G.E. Petrov, G.A. Riabov, V.M. Samsonov, L.E. Samsonov. E.M .Spiridenkov, V.V. Sulimov, O.I. Sumbaev, V.A. Schegel'ski, Pis'ma Zh. Eksp. Teor. Fiz. 36 (1982) 340.
16. P.J.C. King, M.B.H. Breese, P.J.M. Smulders, P.R. Wilshow, G.W. Grime, Phys. Rev. Lett. 74 (1995) 411.
17. J.U. Andersen, Talk at the Memorial Symposium for Jens Lindhard, Aarhus, March 1998.
18. J.F. Ziegler, J.P. Biersack, V. Littmark, Stopping and Range of Ions in Solids, Pergamon, N. Y., 1985.
19. W. Lotz, Z. Phys. 216 (1968) 241.
20. S.K. Allison, Rev. Mod. Phys. 30 (1958) 1137.
21. E. Horsdal-Pedersen, Ph.D.Thesis, Aarhus, 1984.
22. K. Shima, N. Kuno, M. Yamanouchi, At. Data Nucl. Data Tables 51 (1992) 173.

Received by Publishing Department
on August 17, 1999.